Vol. 69: 155–176, 2016
doi: 10.3354/cr01397

CLIMATE RESEARCH
Clim Res

Published online July 27

Dates of frost onset, frost end and the frost-free season in Turkey: trends, variability and links to the North Atlantic and Arctic Oscillation indices, 1950–2013

Ecmel Erlat[1], Murat Türkeş[2,*]

[1]The Physical Geography Division, Department of Geography, University of Ege, 35100 Bornova-Izmir, Turkey
[2]The Center for Climate Change and Policy Studies, Boğaziçi University, Istanbul, Turkey

ABSTRACT: This study examines the climatology, inter-annual variability and long-term trends of dates of the first fall frost (FFF) and last spring frost (LSF) events, and lengths of the frost-free periods (FFP) by using daily minimum air temperature data from 80 stations in Turkey. Influences of the North Atlantic Oscillation (NAO) and the Arctic Oscillation (AO) teleconnection patterns on the variability of these climatic observations are also investigated. A trend towards later FFF and earlier LSF, and a resulting lengthened FFP are detected, with some regional differences, particularly in the Black Sea Region. Linear trend analysis of nationally averaged time series showed that the LSF occurred earlier by −0.64 d per decade, while the FFP occurred later with an increase rate of +0.71 d per decade over the study period. Correlation analysis revealed that year-to-year variations in occurrence dates of FFF, and LSF events and lengths of FFP could be explained by large-scale atmospheric circulation or oscillation patterns such as NAO/AO. Negative relationships were detected between the variability of dates of FFF events over Turkey and autumn indices of the NAO and AO indices. Correlation coefficients were statistically significant at the 1% level for the majority of stations. Positive linkages between the dates of the LSF events and the NAO and AO spring indices were obtained at most of the stations in Turkey. The lengths of FFP also tended to increase during negative NAO/AO index phases, while they tended to decrease during positive phases.

KEY WORDS: Turkey · Climate variability · Frost event climatology · Frost event changes · NAO · AO

1. INTRODUCTION

The most recent Fifth Assessment Report (AR5) of Working Group I of the Intergovernmental Panel on Climate Change (IPCC) concludes globally averaged surface (combined land and ocean) temperatures increased by 0.85°C (range 0.65 to 1.06°C) over the period 1880–2012. The rate of warming over the period 1951–2012 was about 0.72°C (range 0.49 to 0.89°C) (IPCC 2013). Most data sets also indicate that observed surface warming was associated with relatively larger increases in daily minimum night-time air temperatures (T_{min}) than daily maximum daytime air temperatures (T_{max}) over the last 50 yr (e.g. Easterling et al. 1997, Frich et al. 2002, Türke & Sümer 2004, Hansen et al. 2012, IPCC 2013). Among other effects, the warming in T_{min} since the 1950s may has been associated with a shift in frequency distribution of T_{min}-related extremes, such as number of frost and frost-free days, last spring and first fall freeze dates, and growing-season length.

*Corresponding author: murat.turkes@boun.edu.tr

Since the early 1980s, scientific interest in frost indices has increased because they are important indicators of climatic change, and frost has discernible impacts on socioeconomic sectors including agriculture, energy production and consumption patterns, as well as on natural ecosystems. Previous studies have documented considerable changes in the frost indices within Europe. Klein Tank & Können (2003) presented a European-averaged trend of frost days of −1.7 d per decade, with 9.2 fewer frost days in 1999 compared to 1946. Menzel et al. (2003) pointed out that the dates of last spring frost events during the period 1951–2000 advanced by 0.24 d yr^{-1} on average, while dates of first autumn frosts were delayed by up to 0.25 d yr^{-1} and, as a result, the frost-free period lengthened by 0.49 d yr^{-1}, due to an increase in T_{min} rather than in T_{max} (Table 1). Scheifinger et al. (2003) concluded the occurrence date of the last spring frost in Central Europe was increasingly early during the last few decades. Bartholy & Pongrácz (2007) showed a decreasing trend in number of cold nights, severe cold days and frost days between 1961 and 2001 over the Carpathian Basin. Many studies also reported an extended growing season and changed spring phenology mainly caused by the earlier onset of spring (e.g. Menzel & Fabian 1999, Ahas et al. 2002, Qian et al. 2009, Kirbyshire & Bigg 2010, etc.).

Regarding the Eastern Mediterranean and the Middle East regions, Zhang et al. (2005), for example, found a decrease in frost days at 52 stations across the Middle East since the 1980s. Kuglitsch et al. (2010) determined that the warming in T_{min} since the 1950s has likely been associated with a shift in frequency distribution of T_{min}-related variables such as number of frost and frost-free days, last spring and first fall freeze dates and growing season length across the Eastern Mediterranean Basin. Erlat & Türkeş (2012) indicated that the annual number of frost days evidently decreased at most of the stations over Turkey during the period 1950–2010. Results also showed that the decreasing trends in the number of frost days display considerable decadal-scale variability, which may be linked to large-scale atmospheric teleconnections such as the Arctic Oscillation (AO) and/or North Atlantic Oscillation (NAO) and the North Sea-Caspian Pattern.

Projections by both global and regional climate models, based on the different greenhouse gases emission scenarios, also indicate that the considerable changes in surface air temperatures and temperature-related extremes, such as increases in the occurrence of hot days, changes in the length of heatwaves, and decreases in number of frost days will continue in the future with diverse spatial and temporal variations (e.g. Beniston et al. 2007, Giorgi & Lionello 2008, Orlowsky & Seneviratne 2012, Altinsoy et al. 2012, IPCC 2013, Turp et al. 2015, Öztürk et al. 2015, etc.).

However, climatology, long-term variability and trends in the dates of early and late frost events in Turkey have not yet been examined in any peer-reviewed article. Consequently, the present study aims at performing the following:

(1) To provide a comprehensive analysis showing the spatiotemporal variability of the dates of the last spring frosts (LSF) and the first fall frosts (FFF) events, and the length of the frost-free periods (FFP) in Turkey, and to estimate long-term tendencies in regional and station-based series of LSF and FFF events, as well as the length of the FFP.

(2) To analyse the linkages between the patterns of 2 modes of atmospheric circulation, i.e. the AO and the NAO, and series of the LSF and FFF from 80 climatological and meteorological stations in Turkey.

(3) To examine the influence of the anomalous circulation patterns associated with the occurrence of extreme dates of the FFF and LSF events (i.e. earliest or latest) in Turkey.

Table 1. Summary of peer-reviewed scientific literature on changes in frost indices in the long series of the climatological records over the Europe and Middle East. nFD: number of frost days; FFF: first fall frost; LSF: last spring frost; FFP: frost-free period

Frost indices	Region/ country	Time span	No. of stations	Change (d yr^{-1})				Reference
				nFD	FFF	LSF	FFP	
nFD	Europe	1946–1999	195	−0.17				Klein Tank & Können 2003
FFF, LSF, FFP	Germany	1951–2000	41		+0.25	−0.24	+0.49	Menzel et al. 2003
LSF	Central Europe	1951–1997	50			−0.2		Scheifinger et al. 2003
nFD	Middle East	1970–2003	52	−4.7 to −0.7				Zhang et al. 2005
nFD	Turkey	1950–2010	72	−0.4 to +0.19				Erlat & Türkeş 2012

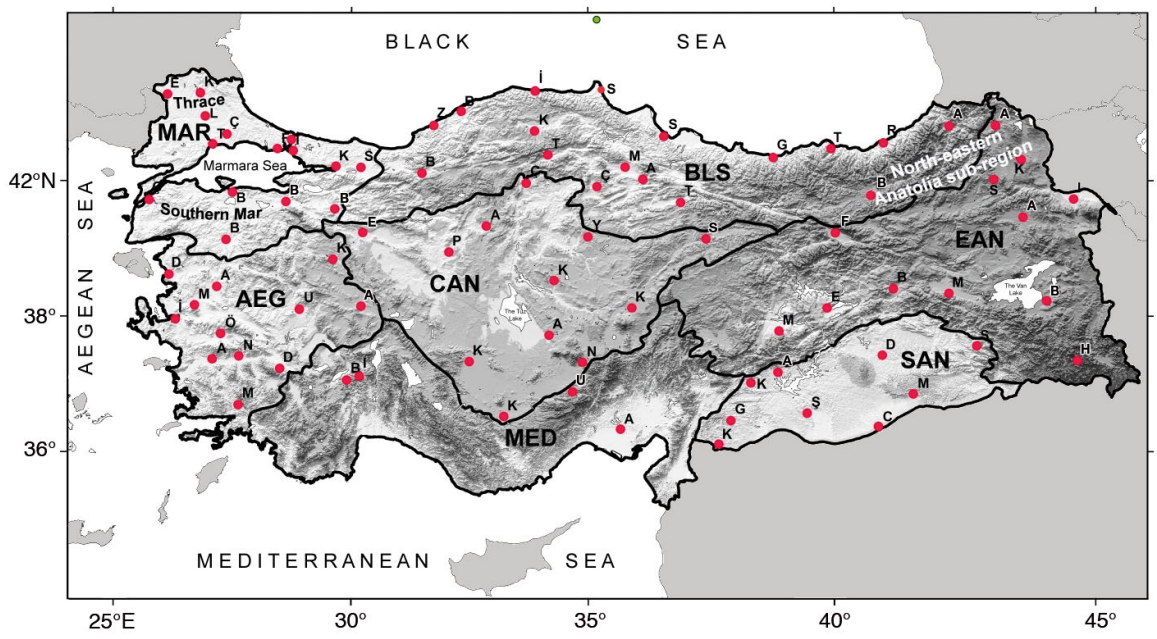

Fig. 1. Spatial distribution of the 80 climatological and meteorological stations (upper-case letters give first letter of meteorological station used) considered in the study of frost event indices of Turkey, superimposed on a physiographic map showing the borders of geographical regions. BLS: Black Sea; MAR: Marmara; AEG; Aegean; MED: Mediterranean; SAN: Southeastern Anatolia; CAN: Central Anatolia, and EAN: Eastern Anatolia

2. DATA AND METHODOLOGY

2.1. Climatological data

We used the daily T_{min} series of Turkey recorded at 80 climatological and meteorological stations of the Turkish Meteorological Service (Fig. 1). Because of the large gaps in daily temperature measurements prior to the 1950s, our analysis focused on the most continuous daily data of the period, 1950–2013. In order to reach a uniform geographical coverage over Turkey, we used 16 stations that only had records covering the period 1960–2013. To select the stations, we applied the rules that a candidate station should have almost complete daily temperature data (with <5% missing or unusable data) in the cold season of a given year. A very small number of missing daily data at some stations was filled using a simple approach of averaging the 2 values of the previous and later days with respect to the day of missing value, based on the basic weather information indicating the autocorrelation characteristic of daily air temperature series. The selected stations were distributed among the 7 geographical regions of Turkey: Black Sea (BLS), Marmara (MAR), Aegean (AEG), Mediterranean (MED), Southeastern Anatolia (SAN), Central Anatolia (CAN), and Eastern Anatolia (EAN) (Fig. 1). According to Digital Elevation Model (DEM) analysis, the elevation of 33 stations is below 500 m, while the elevation of 27 stations ranges from 500 to 1000 m. The elevation of 20 stations is above 1000 m, of which 7 are above 1500 m. Most of the stations located on the Turkish coastal belts of the Aegean and the Mediterranean seas were not included in the present study, because the frost events on these coastal stations are very rare and random, and not suitable for such climate variability and trend analyses. Therefore, those stations were not able to be used in any part of the analysis (neither station-based nor regional).

Quality and homogeneity controls of air temperature series were checked using various statistical and graphical techniques, making use of a station history file developed by Türkeş et al. (2002a) and Türkeş (2013) for about 80 and 140 stations of Turkey, respectively. A total of about 140 candidate stations were reexamined with respect to their record length, data gap, geographic representativeness over Turkey, and inhomogeneity, i.e. the occurrence of marked non-climatological jumps (abrupt or step-wise changes) in the mean of the series. In order to detect homogeneity in daily and monthly T_{min} series, first a homogeneity analysis was performed by using the non-parametric Kruskal–Wallis and runs tests. Second, the non-parametric Wald–Wolfowitz serial correlation test was applied to the series to examine the nature and magnitude of the serial dependence and/or abrupt

changes in the series (Sneyers 1990, Türkeş et al. 2002a). Finally, after checking statistically significant inhomogeneity results from the tests against additional information from our station's history file and the plotted time-series, we selected the daily T_{min} series for a total of 80 meteorological stations. Detailed information on homogeneity and other time-series characteristics of Turkish air temperature data can be found particularly in Türkeş et al. (2002a). The geographical distributions of the climatological and meteorological stations used in the study are shown on a physiographic map of Turkey in Fig. 1.

Table 2. Definitions of the indices used in the present study. T_{min}: minimum air temperature

Abbreviation	Indices	Definition	Unit
FFF	First fall frost	The first date in a year after July 1 on which $T_{min} \leq 0$°C	Day of the year
LSF	Last spring frost	The last date in a year on, or before, June 30 in which the daily $T_{min} \leq 0$°C	Day of the year
FFP	Frost-free period	The number of days between the last spring frost day and the first fall frost day	d

We define a frost day as a day with $T_{min} \leq 0$°C. We also used a threshold of 0°C for daily T_{min} to determine changes in dates of the first-autumn and last-spring frosts, and length of the frost free season. The first-autumn and last-spring frost dates were converted to day-of-the-year values. In some years and at some stations, the first-autumn frost date occurs after 1 January or last-spring frost dates occur prior to 1 January. Because of this, we recognize 1 July as the date dividing spring and autumn seasons. Accordingly, we defined FFF as the first day when $T_{min} \leq 0$°C in the period starting on 1 July, and LSF as the last day when $T_{min} \leq 0$°C in the period ending on 30 June (Table 2). Finally, we calculated anomaly time series of FFF, FSF and FFP for each of the climatology/meteorology stations selected.

2.2. Synoptic climatological and atmospheric oscillation index data

The NAO and the AO indices were employed to investigate the potential causes of the year-to-year variability in the FFF, LSF dates and length of FFP from 1950 to 2013. The NAO monthly index data (based on Gibraltar and Reykjavik) for the period 1950–2013 was taken from the Climatic Research Unit (www.cru.uea.ac.uk/~timo/datapages/naoi.htm). Time series of daily AO index from 1950 was derived from the Climate Prediction Center of the National Centers for Environmental Prediction at the NOAA National Weather Service (CPC/NCEP/NOAA, 2014; www.cpc.ncep.noaa.gov/products/precip/CWlink/daily_ao_index/monthly.ao.index.b50.current.ascii.table). In order to investigate the upper atmospheric meteorological conditions that may have controlled the variability and extreme states of the frost events in Turkey, we used NCEP/NCAR reanalysis derived data (Kalnay et al. 1996). The NCEP/NCAR Reanalysis 1 (R1) dataset was provided by the NOAA Earth System Research Laboratory, Physical Sciences Division from their website at www.esrl.noaa.gov/psd/, and we also made use of their map producing tools for our northern hemispheric scale synoptic climatological composite analysis from the website at www.esrl.noaa.gov/psd/data/gridded/data.ncep.reanalysis.html. The atmospheric data we used contains the 500 hPa standard pressure level geopotential heights (m), 850 hPa standard pressure level air temperatures (°C), and meridional and zonal wind speeds ($m\ s^{-1}$) at the 500 hPa standard pressure level.

The length and time range of our study period is obviously the main reason to use the R1 dataset. There are multiple comparison studies and comparable information for various reanalysis-derived datasets for different variables in the literature, and often one reanalysis dataset is better than another for one type of variable (or one region) but not for another (or another region) (e.g. Smith et al. 2014, www.esrl.noaa.gov/psd/data/writ/ or https://reanalyses.org). In this respect, we made some comparisons among the long-term average and composite anomaly conditions of the data used in the study for a common length of period. Even though we detected some differences among them, the differences between NCEPR1 and other datasets (i.e. JRA55 and the ERA Interim that started in 1958, and the NCEP/DOE Reanalysis II [R2] started in 1979) are not sufficiently great over Turkey and its region to affect our analysis in terms of the synoptic scale weather systems (results not shown).

2.3. Methods

The non-parametric Mann–Kendall rank correlation test was performed to detect any possible trend in the station-based, and regionally and nationally averaged

time-series of the frost events in Turkey, and to test whether such trends are statistically significant or not (WMO 1966). Using critical values from a 2-sided test of the normal distribution, which is equal to 1.96 and 2.58 for the 5 and 1% levels of significance, respectively; a null hypothesis of absence of any trend in these series is rejected for the large values of the calculated Mann-Kendall statistic $(\tau)_t$ regarding the desired level of significance (Türkeş et al. 2002a).

The least squares linear regression (LSLR) equation was also calculated to estimate the trends rates in the FFF, LSF and FFP series for both individual station time-series and national and regional time-series, with time as the independent variable and the FFF, LSF and FFP values as the dependent variables. The statistical significance of each estimated β coefficient was tested by the Student's *t*-test with (n – 2) degrees of freedom. Using a 2-tailed test of the Student's *t*-distribution, the null hypothesis — the absence of any linear trend in the time-series — was rejected in accordance with the large *t*-test values (Türkeş & Sümer 2004).

Pearson correlation (r) analysis was made between the index series of the AO and NAO and the series of the LSF and FFF from the 80 climatological and meteorological stations of Turkey, in order to detect relationships (control mechanisms) between year-to-year variability of these teleconnection patterns and the occurrence dates of frost events in Turkey. Statistical significance of the correlation coefficient r was checked by using a 2-tailed test of the Student's *t*-distribution; the null hypothesis — the absence of any correlation between AO/NAO indices and series of frost event dates in Turkey — was rejected in accordance with the large values of Student's *t*-statistic (Erlat & Türkeş 2012). Both 0.05 and 0.01 levels of significance (i.e. 0.95 and 0.99 confidence levels) were mostly used for the tests of hypothesis in the study.

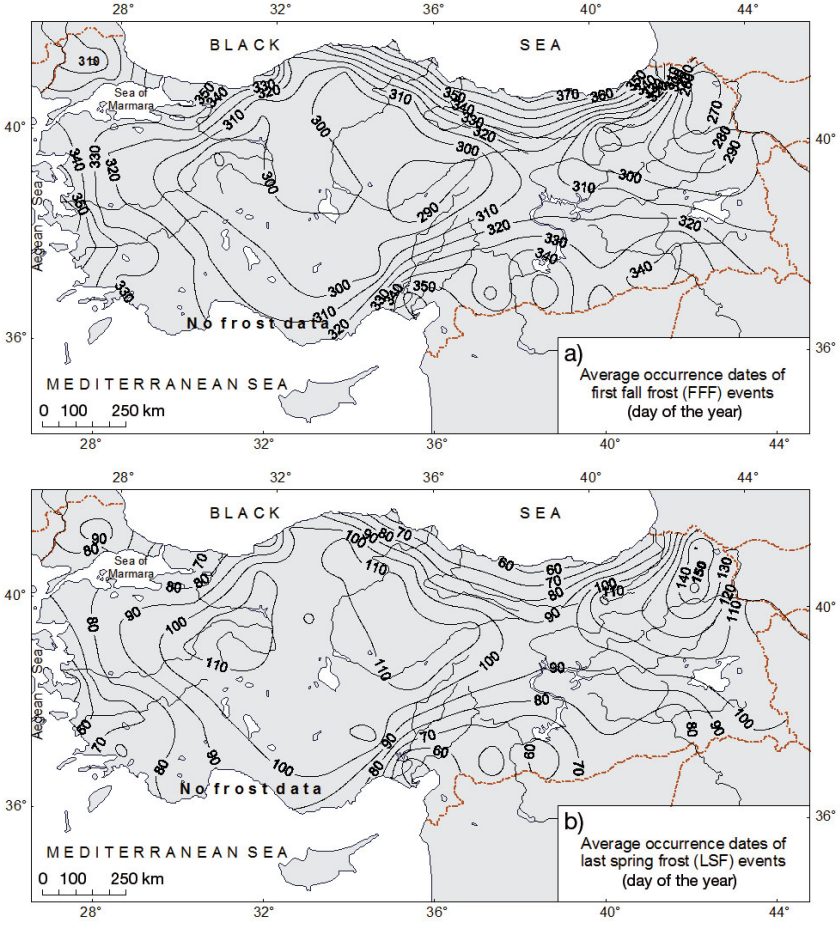

Fig. 2. Geographical distribution patterns of the long-term average occurrence dates of (a) first fall frost (FFF) and (b) last spring frost (LSF) events, according to the daily minimum air temperature (T_{min}) data recorded at the 80 climatological/meteorological stations of Turkey during the period 1950–2013

3. RESULTS AND DISCUSSION

3.1. Climatology of frost dates and periods in Turkey

The spatial patterns of the average occurrence dates of FFF, LSF and lengths of FFP are geographically highly variable due to the factors linked to atmospheric circulation patterns and synoptic-scale weather systems, as well as physical geographical features including continentality and the topographic/geomorphologic characteristics of Turkey.

First frost dates that occur mainly in the fall season and partly in the early winter exhibit a high spatial variability in Turkey. Earliest occurrence of the FFF events is seen across the mountainous portions of eastern and northeastern Anatolia regions of Turkey (Fig. 2a). The long-term average dates of the FFF vary between Days 270 and 290 (i.e. late September and mid-October). The average onset date of fall frost appears at Day 261 (18 September) at Ardahan over the northernmost part of the northeastern Anatolia sub-region, where the station altitude is 1800 m. In the continental central Anatolian plateau, the

FFF occurs between Days 280 and 300; in October. There is clear evidence of an increasing delay in the FFF, moving from the continental inner regions of the country to maritime/temperate coastal areas. The first frost events occur as late as Days 360 and 380 (mid-December and mid-January — i.e. Day 15 of the following year) on the Mediterranean Sea and Black Sea coastal belts of Turkey and the Aegean region, respectively. For instance, the average date of the FFF is Day 15, in January, at Sinop station located on the mid-Turkish Black Sea coast (Fig. 2a).

Spatial distribution patterns of LSF are highly variable and range from Days 150 to 40. Latest average LSF dates are recorded in Eastern and northeastern Anatolia, where LSF occurs most frequently between Days 150 and 130 (Fig. 2b). The average date of LSF is Day 156 (30 May) at Sarıkamış station located in EAN in the continental northeastern Anatolia sub-region. In the continental CAN, average dates of LSF fall between Days 100 and 140 (i.e. mid-April and mid-May). The earliest average LSF dates occur on the Mediterranean and Aegean coasts of Turkey (i.e. mid-February to mid-January); for example, the average date of occurrence of the LSF is on Day 40 at the Adana and Ízmir stations (Fig. 2b).

The average lengths of the FFP in Turkey reveal an apparent regional difference (Fig. 3a) between maritime/temperate coastal regions and continental/cold inner and higher regions of Turkey. For the coastal areas of Turkey, FFP values range from 330 d on the Black Sea coast to 280 d along the coast of the Aegean Sea. The Mediterranean coasts of Turkey are mostly frost free. In the continental CAN, the frost-free period at 1000 m above mean sea level is about 150 to 180 d. Higher altitudes and the mountainous northeastern Anatolia sub-region of the Anatolian Peninsula may experience <120 d frost-free, as in Sarıkamıs¸ station, where this figure is 105 d (Fig. 3a). The geographical distribution pattern of the year-to-year variability in the series of FFF, LSF and FFP were investigated by using the percentage coefficient of variation (CV). The CV statistic is computed by expressing long-term standard deviation as a percentage of the long-term average of the series. CVs of the FFF, LSF and FFP reveal a similar pattern of variation from the most continental and the highest altitude parts of cold northeast Anatolia towards the southernmost coastal regions characterised by a subtropical maritime/temperate Mediterranean climate. We display here only the map of CV for the FFP (Fig. 3b). The CV of FFF over Turkey ranges from 3.5% in the continental north-eastern part of the Anatolian Peninsula to 6.5 to 7.0% on the Aegean and Mediterranean coasts (results not shown). Inter-annual variations of the LSF are higher than for FFF. The CV of LSF decreases from the temperate coastal and southern regions to the continental and cold interior and northeastern Anatolia (data not shown). The lowest year-to-year variability is about 10% at the stations of the continental eastern and northeastern parts of the Anatolian Peninsula. The CV of LSF reaches 60% on the Black Sea coasts. The largest year-to-year variability in the frost

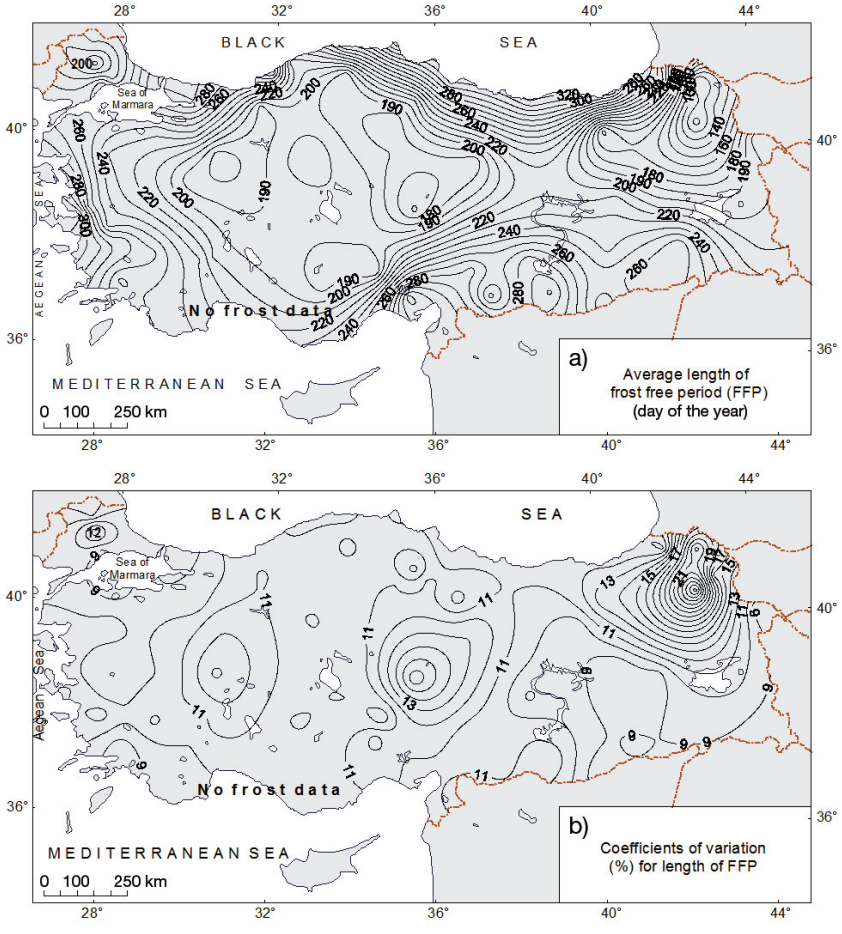

Fig. 3. Geographical distribution patterns of (a) long-term average lengths (d) of the frost-free period (FFP) in Turkey and (b) coefficients of variation (CV, %) of the lengths of the FFP

free period is detected in the areas where FFF dates and LSF dates also exhibit high variability.

Inter-annual variability of the lengths of the FFP increases from the maritime/temperate coastal southern regions, characterised by dry, hot summers typical of a subtropical Mediterranean climate, to the continental cold northeastern Anatolia sub-region of the country (Fig. 3b). Lowest CV values are found over the SAN and AEG regions. For instance, Ceylanpinar station located on the border of Turkey and Syria shows a CV of 8.1%, whereas higher inter-annual variability is the norm over the continental cold CAR and the northeastern Anatolia sub-region of the country; for example at Sarıkamış, where the CV of FFP is 26.6% (Fig. 3b).

3.2. Long-term variations and trends in the dates of first fall frost events

Graphical and statistical time-series analyses were performed to elucidate long-term trends in nationally averaged series for FFF, LSF and FFP events (Fig. 4, Table 3) and trends in the regionally averaged series of the 7 geographical regions that characterise the main climate types in Turkey, i.e. humid-temperate (BLS), Mediterranean (AEG and MED), continental steppe (CAN), continental cold (EAN) and continental Mediterranean (SEA) (Fig. 5, Table 3). Using series of the geographical regions is the most practical way to present regional climatic features; however there are more than 7 climate types in Turkey. For instance, more than 12 climate types can be identified based on the multivariate cluster techniques (e.g. Fahmi et al. 2007, Şahin & Cigizoglu 2012, Iyigün et al. 2013). Due to space considerations, we limit ourselves to briefly summarising the results of the trend test statistics (Table 3); we provide graphical representations of time-series for the 7 geographical regions and 3 frost event variables in graphical form (Fig. 5).

Time series of nationally averaged values of the dates of FFF events shows a high interannual and decadal variability during the study period 1950–2013 (Fig. 4a). Although observed trends in all frost event indices of Turkey (Fig. 4) are not statistically significant according to the Mann–Kendall test (Table 3), there are some distinct periods that can be defined in the time series of the FFF events. Generally, from 1950 to 1977, the occurrence dates of FFF events showed greater interannual variability. For instance, the years of 1952 and 1966 were characterized by latest FFF dates at most of the stations. On the other hand, the years of 1956 and 1973 were characterized by earliest FFF dates for most of the stations. During the period 1978–1994, the FFF dates were earlier or near the long-term average and characterised by lower year-to-year variability. After the year 1995, FFF events mostly occurred later compared with the long-term average. For instance the years of 1998, 2009 and 2010 were characterized with

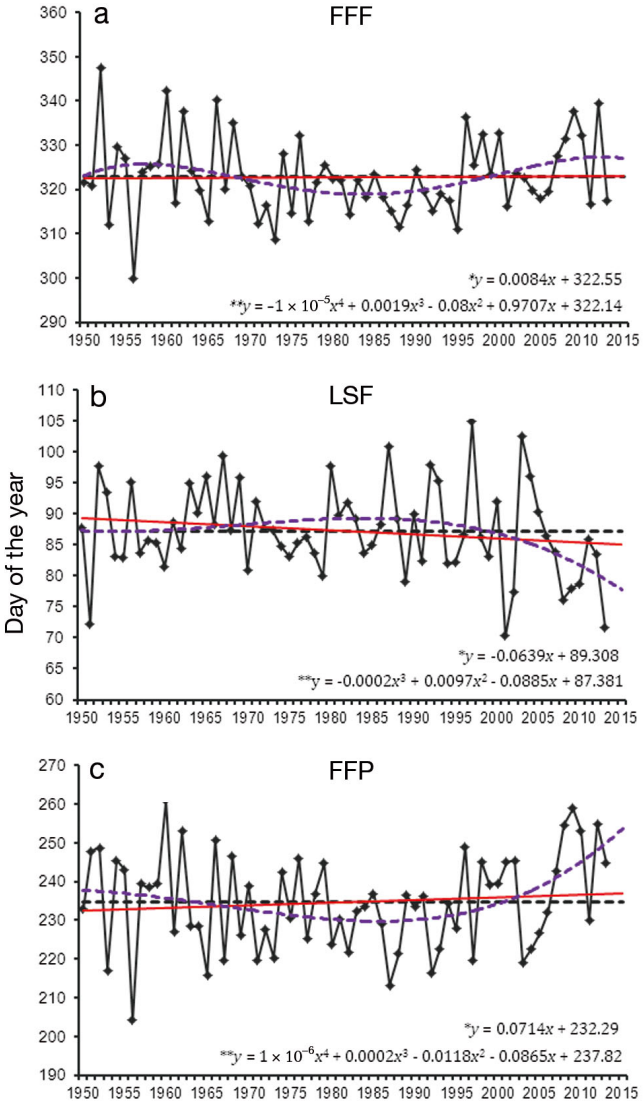

Fig. 4. Long-term variations in nationally averaged time series for (a) first fall frost (FFF), (b) last spring frost (LSF) and (c) the frost-free period (FFP) in Turkey during 1950–2013, relative to long-term averages (black dashed line) and trends in polynomial (4th, 3rd and 4th degree polynomial regression fits; a, b and c, respectively — purple dashed curves) and simple linear least-squares linear regression fits (red straight lines). The equations of polynomial and least-squares linear regression models are displayed in the respective panels

Table 3. Test statistics $u(t)$ of the Mann–Kendal rank correlation coefficient analysis and the Student's t-statistics for the significance of regression coefficient (β), derived from the least squares linear regression equation LSLRE) applied to regional and national FFF, LSF and FFP series (see Table 2) of the geographical regions and the whole of Turkey, respectively. See Fig. 1 for abbreviated names of regions. p_{ht}: probability results of the hypothesis tests indicating statistically significant trends at the *10%, **5% and ***1% significance level

Area and index	Mann–Kendall $u(t)$	p_{ht}	β of LSLRE t	p_{ht}
Turkey				
FFF	0.14		0.03	
LSF	−1.30		−1.37	
FFP	0.85		0.67	
BLS				
FFF	−1.68	*	−1.51	
LSF	1.65	*	1.19	
FFP	−2.28	**	−1.96	**
MAR				
FFF	−0.42		−0.43	
LSF	−4.05	***	−4.10	***
FFP	1.92	*	1.45	
AEG				
FFF	0.82		0.68	
LSF	−2.83	***	−2.73	***
FFP	2.40	**	1.99	**
MED				
FFF	−1.02		−0.46	
LSF	−0.78		−0.67	
FFP	−0.59		0.22	
SAN				
FFF	1.71	*	1.71	*
LSF	−1.29		−1.65	*
FFP	2.00	**	1.95	*
CAN				
FFF	1.92	*	2.11	**
LSF	−1.38		−1.22	
FFP	2.77	***	2.95	**
EAN				
FFF	0.91		1.00	
LSF	0.53		0.19	
FFP	0.05		0.37	

later dates for FFF at many of the stations. Regionally, the observed decreasing trend in BLS is statistically significant at the 0.10 level of significance, while the SAN and CAN show a significant increasing trend at the 0.10 level (Fig. 5 and Table 3).

The Mann–Kendall test statistics calculated for station-based time-series reveal that FFF is characterized with a general positive trend over much of Turkey. FFF occurred later at 52 of 80 stations over the study period (Fig. 6a). For the 1950–2013 period, FFF increased significantly at 14 stations, 8 of which are significant at the 0.01 level, and 6 at the 0.05 level. The low number of stations with significant trends is due to high interannual variability. The annual increasing trends are highest over the continental CAN, SAN and EAN regions (Fig. 6a).

Although the nationally averaged time series of FFF show somewhat high variability over their long-term averages rather than indicating a statistically significant trend over their long-term averages, we performed both parametric polynomial and simple LSLR analysis for these series in order to show long-term trends and detect the rate of changes in the variables through the study period, respectively (Fig. 5). A simple LSLR model applied to the annual averages of Turkey as a whole revealed a trend of slightly later occurrence of FFF, with a low rate of increase rate of +0.1 d per decade over the study period. Linear trend estimations (maps of test statistics and trend rates derived from the LSLR analysis not given here) for some locations, such as Gaziantep reveals a positive trend of 5 d per decade. Similarly, positive trends range from 3.2 (Konya) to 2.8 d per decade (Iğdir), in stations located in the continental and cold CAN and EAN regions of Turkey, respectively. On the Black Sea coast, as we have already pointed out above for the regional BLS series, the observed trends are opposite to the trend patterns over the rest of Turkey (Fig. 6a). This differentiation is mainly due to various atmospheric circulation patterns and synoptic-scale weather systems (e.g. mid-latitude cyclones, upper atmospheric level troughs and lows) leading to different weather and climate mechanisms and conditions in the BLS region (Kutiel & Türkeş 2005, Türkeş 1998, Türkeş et al. 2002b, Türkeş & Erlat 2008, 2009, Iyigün et al. 2013, Şahin & Türkeş 2013).

3.3. Long-term variations and trends in the dates of last spring frost events

Long-term variations in the nationally averaged occurrence dates of LSF events in Turkey are characterised by a markedly high interannual and decadal variability between 1950 and 2013 (Fig. 4b). During the period 1950–1979, occurrence dates of the LSF events revealed generally long-period fluctuations; whereas, after the year 1979, LSF events showed relatively higher variability with respect to the long-term average. For example, the year of 1997 was characterized with later dates for the LSF at many of the stations. After 2000, LSF events generally occurred earlier with a distinct reversal in 2001.

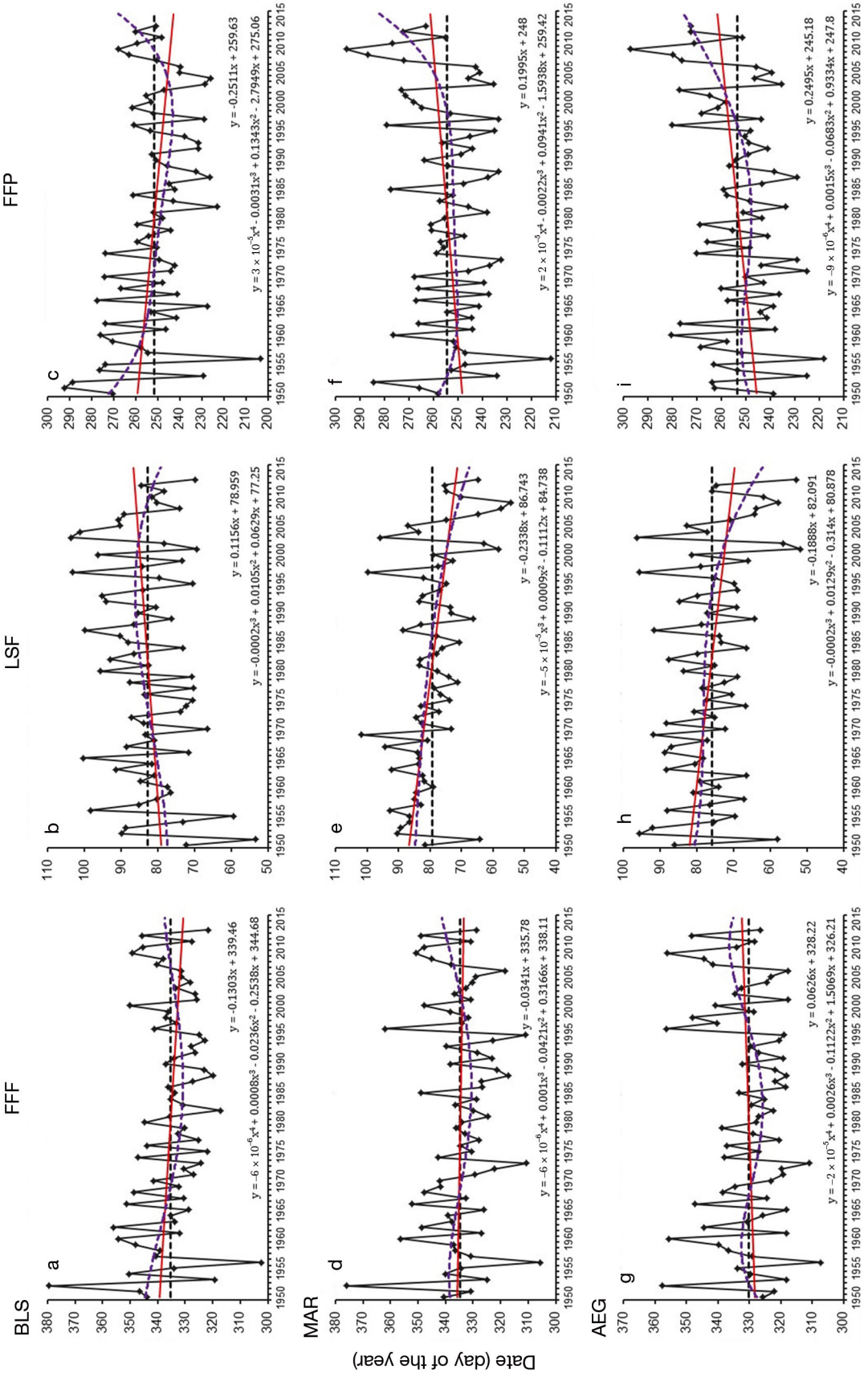

Fig. 5. Long term variations in averaged frost event data in geographical regions of Turkey (see Fig. 1) relative to long-term averages and trends in polynomial and least-squares linear regression fits. See Fig. 4 legend for further details

(Fig. 5 continued on next page)

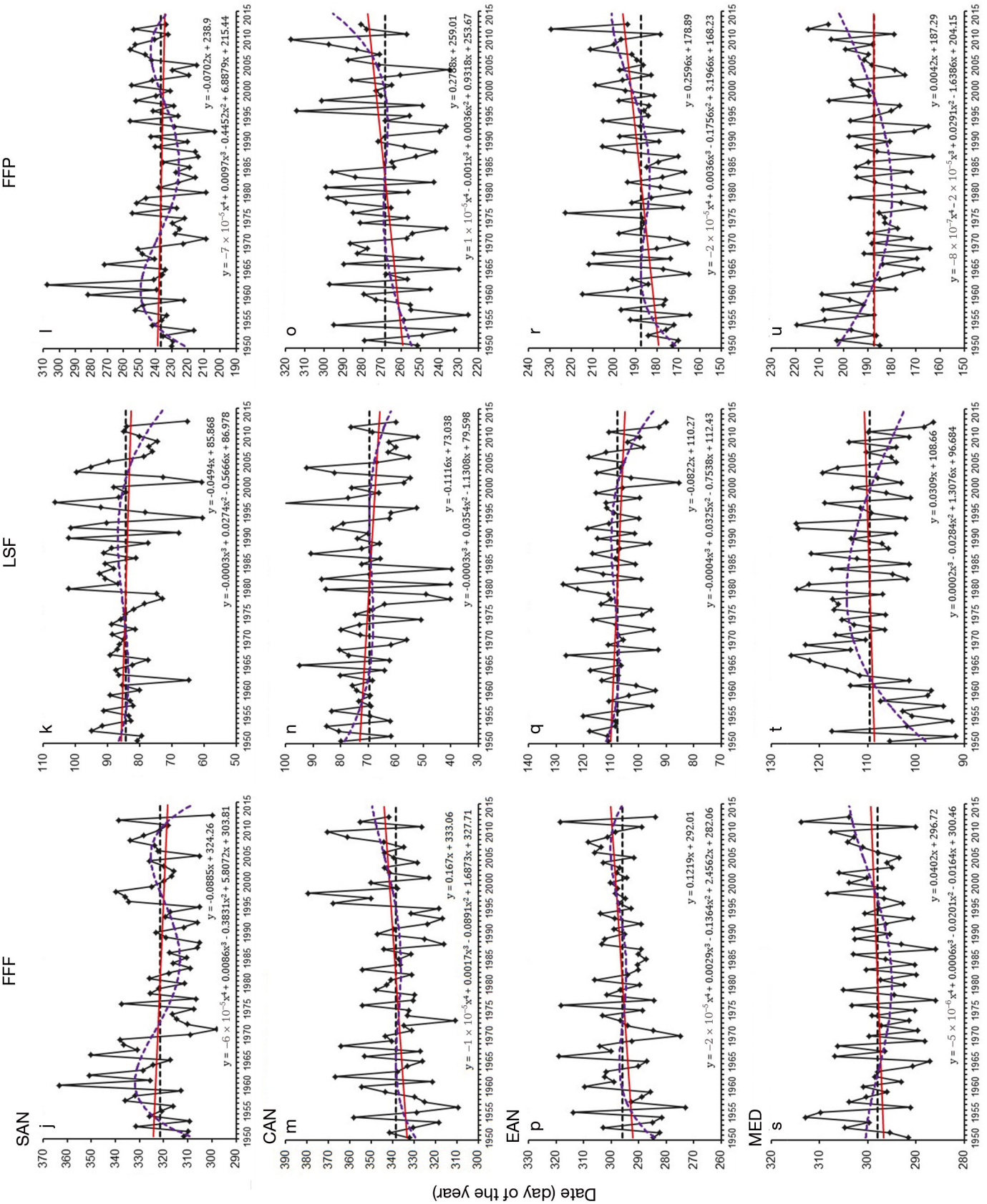

Fig. 5 (continued)

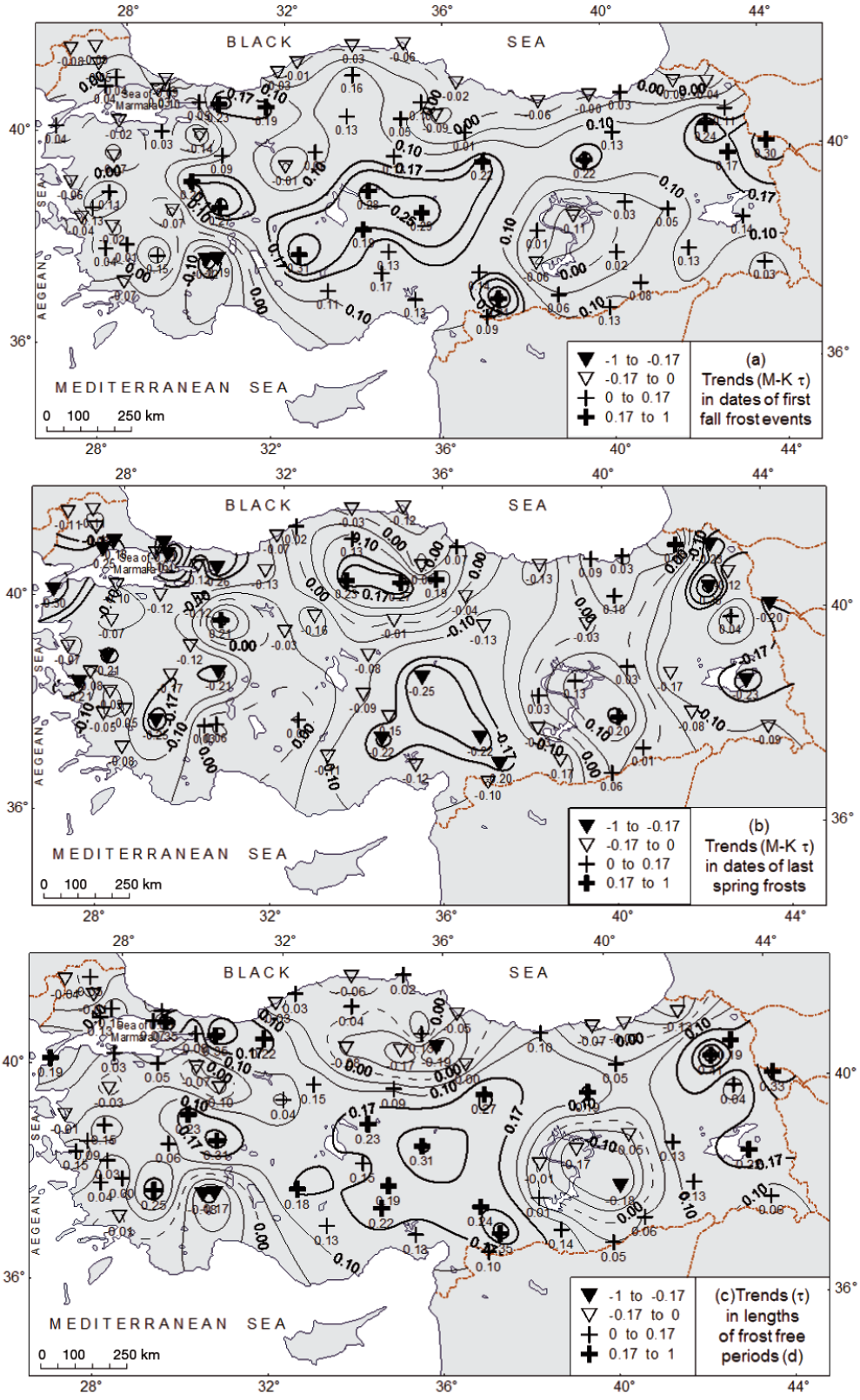

Fig. 6. Spatial distribution patterns of the Mann–Kendall rank correlation coefficients over Turkey, calculated for frost event indices (a) FFF, (b) LSF, and (c) FFP for the period 1950–2013. Triangles represent negative (decreasing) and plus symbols represent positive (increasing) trends, respectively. Solid triangles, bold plus symbols and bold lines represent statistically significant trends at the 5% level of significance, which are displayed in the key

In that year, the date of LSF events generally occurred earlier than long-term average conditions across Turkey. The LSF series of the BLS region showed a significant increasing trend at the 0.10 level, in contrast to the LSF series of the MAR and AEG regions, that showed a significant decreasing trend at the 0.01 level (Fig. 5, Table 3).

The results of the Mann–Kendall test indicated that the occurrence dates of LSF events have shifted to an earlier date for most of the stations in Turkey considered in the study (Fig. 6b). Dates of the LSF events display a notable decreasing trend at 59 of 80 stations over the study period, which is statistically significant at 17 stations (8 stations at the 0.01 level and 9 stations at the 0.05 level). For example, the dates of LSF events showed a linear shift to an earlier date at a rate of about −7.7 d per decade at Istanbul (Göztepe-Kartal), and −7.5 d per decade at Sarıkamış. According to the linear trend analysis of nationally averaged time series, LSF also occurred earlier over the country as a whole, decreasing by −0.64 d per decade over the study period. By contrast, markedly increasing trends in the dates of LSF events were detected at 21 stations; in 5 cases these were statistically significant (Fig. 6b).

3.4. Long-term variations and trends in the lengths of frost free period

Between the mid-1950s and the mid-1960s, the FFP was generally longer than the long-term average, with later FFF and earlier LSF dates. From mid-1960s to mid-1990s, the FFF arrived early and the LSF came later, producing shortened FFP length except during 1975–1980 (Fig. 4c). After the mid-1990s, except in the first few years of the 2000s, the FFP increased markedly due to the contributions of both later FFF and earlier LSF dates. For instance, according to the national averages, the longest lasting FFP occurred in the years of 2009 (258.8 d), 2012 (254.9 d), and 2008 (254.5 d). As for the geographical regions, the FFP series of the BLS region shows a significant decreasing trend at the 0.05 level that is evidently opposite to the other regions in terms of the direction of the observed trend, while the observed increasing trends in the regional FFP series are significant for MAR at the 0.10 level, AEG and SAN at the 0.05 level, and the CAN at the 0.01 level (Fig. 5, Table 3).

The results of the Mann–Kendall test reveal that the rates of change in the lengths of the FFPs per year are positive for the 58 stations, and statistically significant for 21 of these (Fig. 6c). On the other hand, decreasing trends in FFP were evident at 22 stations; however these were statistically significant at only 4 of these, located across different parts of Turkey (Fig. 6c). Linear trend analysis of nationally averaged time series (Fig. 5c) showed that the FFP occurred later, with an increase rate of +0.71 d decade^{-1} over the study period. The largest trend ranges were found at stations in the continental/cold CAN and EAN regions. The Sarıkamış station located in the northeastern Anatolia sub-region (see Fig. 1) showed the highest increase in the lengths of FFP with a rate of change of 10.9 d decade^{-1}.

In order to make a detailed assessment of changes in the length of the FFP, we evaluated the results of the Mann–Kendall test for the occurrence dates of FFF and LSF events together. This analysis showed that FFF tended to occur on later dates, while LSF shifted to an earlier date at 40 out of 80 stations over the period 1950–2013. As we expected, these conditions generally resulted in a significant increase in the length of FFP. The length of FFP showed an increasing trend at 12 stations where LSF occurred earlier but FFF was unchanged. However, none of these were statistically significant. Six stations showed non-significant increasing trends in the FFP where FFF occurred later but LSF was unchanged.

4. ASSOCIATIONS BETWEEN FROST EVENT INDICES IN TURKEY AND NORTHERN HEMISPHERIC ATMOSPHERIC TELECONNECTIONS

In this Section, we analyse and discuss the influence (and interactions) of the year-to-year variability of two of the northern hemispheric atmospheric oscillations (i.e. AO and NAO) and large-scale atmospheric anomalous circulation patterns on the variability and extremes of the frost date events in Turkey.

4.1. Relationships between inter-annual variability of the AO/NAO indices and frost event indices of Turkey

Correlation analysis was performed to assess the strength and direction of the relationships between year-to-year variability of the frost date indices (i.e. dates of FFF and LSF events and length of FFP) and two atmospheric oscillation patterns (NAO and AO). Pearson correlation coefficients (r) were calculated separately for each of the AO and NAO indices (Table 4; see Figs. 7–9 below).

Table 4. Results of correlation analysis between the nationally averaged series of the frost indices FFF, LSF and FFP (see Table 2) and North Atlantic Oscillation (NAO) and Artic Oscillation (AO) indices for the period 1950–2003. Autumn, spring and annual series of NAO/AO indices are considered for FFF, LSF and FFP, respectively. Significant results at the 0.05 level are shown in bold. SON: September–November; SOND: September–December; MAM: March–May; FMAM: February–May

FFF		LSF		FFP	
Period	Pearson's *r*	Period	Pearson's *r*	Period	Pearson's *r*
NAO					
SON	**–0.30**	MAM	0.21	Annual	–0.29
SOND	**–0.37**	FMAM	0.19		
AO					
SON	**–0.49**	MAM	0.17	Annual	–0.28
SOND	**–0.55**	FMAM	0.12		

Correlation coefficients revealed negative relationships between the dates of FFF events and the autumn index values for September–November (SON) and September–December (SOND) of the NAO and AO in Turkey (Tables 4 & 5). This means that FFF events tended to occur on earlier (later) dates during the high (low) index NAO/AO phase. Variability in dates of the FFF events associated with the variability in the autumn AO indices are apparently stronger than those found for the autumn NAO indices and show a much greater spatial coherence over Turkey as a whole. Statistically significant correlations for the AO_{SON} (AO_{SOND}) were detected at 36 (44) stations; 17 (28) of these negative correlations were significant at the 0.01 level. The strongest correlations of AO_{SOND} indices reach –0.5 at a few stations including Bilecik and Bursa, both of which are located geographically in the south-eastern part of the MAR region (Fig. 7a,b).

NAO and AO spring indices for March–May (MAM) and February–May (FMAM) were positively correlated with the dates of the LSF events at most stations in Turkey, but the correlation coefficients were mostly weak (Table 4, Fig. 8a,b). This means that LSF tended to occur at later dates during the positive phases of the spring NAOI/AOI indices and vice versa. The analysis suggests a positive relationship between NAO_{MAM} (NAO_{FMAM}) indices and LSF dates at 66 (59) of the 80 stations, 3 (8) of which are characterised by statistically significant correlations at the 0.05 significance level. Approximately the same correlation pattern was obtained for the spring AO indices.

Previous studies also indicated that positive phases of both the cold season NAO and AO indices are closely associated with anomalous high pressure conditions in southern and central Europe, the Balkans and western Turkey, and thus spatially coherent and significant cold signals dominate over the majority of Turkey. By contrast, during the negative phases of the cold season NAO/AO indices, spatially coherent and significant warm signals over the Anatolian Peninsula appear (Türkeş & Erlat 2008, 2009). As noted by Castro-Diez et al. (2002), the influence of the NAO on temperature variability over Southern Europe is more complex than over Central and Northern Europe, being extremely sensitive to the location of sea level pressure (SLP) anomaly centres. Recent studies also showed that NAO events could be divided into eastern type (ENAO) located east of 10°W and western type (WNAO) located west of 10°W, according to the zonal position of the northern centre of the NAO dipole mode (Yao & Luo 2014). Analysis of the daily NAO index suggests that the eastward shift of NAO events (when the NAO/NAO+ dipole mode is located closer to the European continent) has a greater influence than western type WNAO on the European air temperature. A notable positive temperature anomaly can be observed in the Central and Eastern European regions during the ENAO+ life cycle. By contrast, a negative temperature anomaly is found over Europe during the life cycle of NAO events. The zonal wind over the Atlan-

Table 5. Numbers of stations where significant correlations at the 5 and 1% levels of significance were detected between AO and NAO indices and frost event indices for the period 1950–2013. Abbreviations as in Table 4

FFF				LSF				FFP			
Index and period	Pearson's *r* Negative			Index and period	Pearson's *r* Positive			Index and period	Pearson's *r* Negative		
	5%	1%	Total		5%	1%	Total		5%	1%	Total
AO_{SON}	19	17	36	AO_{MAM}	5	1	6	AO_{ANN}	9	4	13
AO_{SOND}	16	28	44	AO_{FMAM}	3	1	4				
NAO_{SON}	8	11	19	NAO_{MAM}	3	0	3	NAO_{ANN}	12	3	15
NAO_{SOND}	12	15	27	NAO_{FMAM}	7	1	8				

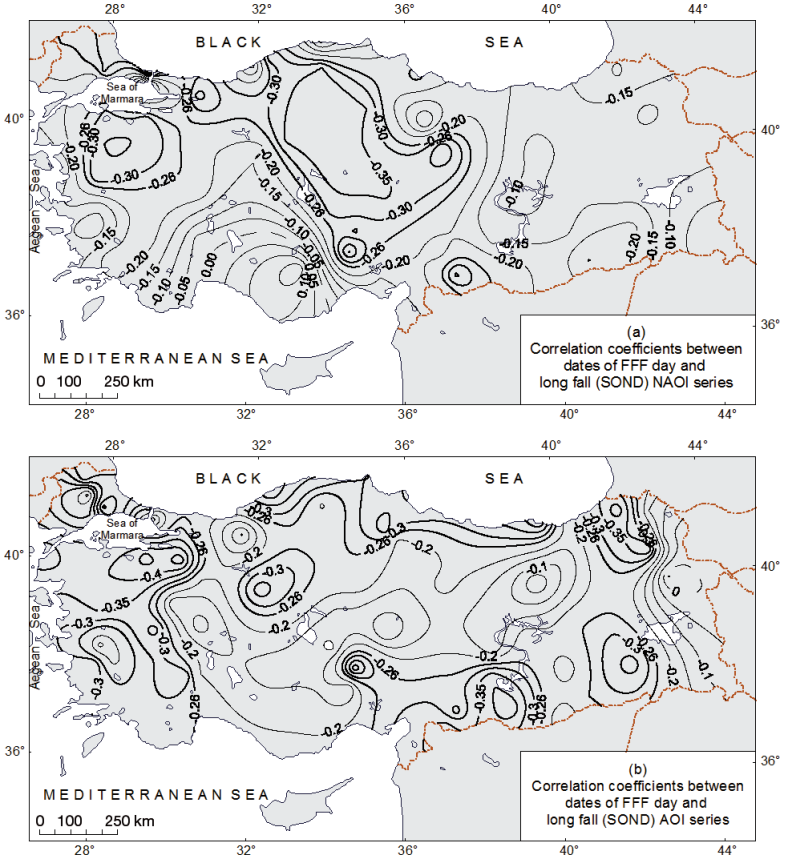

Fig. 7. Geographical distribution patterns of correlation coefficients between the year-to-year variability in occurrence dates of FFF events and the variability in the autumn series (SOND) of the (a) NAO and (b) AO indices. Thick lines represent the areas characterized with statistically significant correlations

tic Ocean during the ENAO events is stronger in mid to high latitudes (40° to 70° N) than during WNAO events (Yao & Luo 2014). Results of Yao & Luo (2014) indicated that the mechanism linking frost event indices over Turkey and these 2 climate oscillations changes with the location of the SLP anomaly centres, especially between the ENAO and WNAO events.

On the other hand, relationships between lengths of FFP and the NAO/AO annual indices are characterised by negative correlation coefficients at many stations considered in this study (Table 4, Fig. 9a,b). According to the significance test of the correlation coefficients, significant relationships were detected between the annual NAO index and FFP at 15 of the 80 stations. Weak relationships between frost indices and the AO/NAO indices can generally be explained by the fact that teleconnection patterns such as the NAO and AO have less influence on the main characteristics of the atmospheric circulation conditions over the Eastern Mediterranean, Levantine and Turkey regions in the summer. In addition to the influences and/or controls arising from regional and local scale atmospheric conditions and weather events in the warm/hot period of the year, a considerable part of the variability in summer atmospheric circulation and weather conditions can be closely linked to the expanded tropical circulation and the Asiatic monsoon low, causing warm season migration of the intertropical convergence zone towards the subtropical zone, including the wider Mediter-

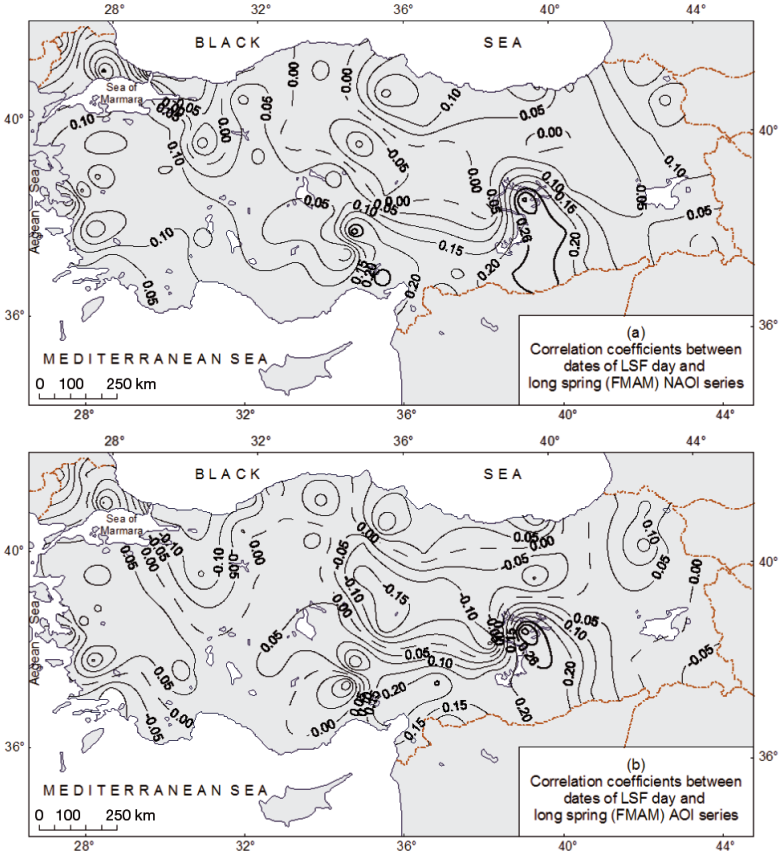

Fig. 8. Geographical distribution patterns of correlation coefficients between the year-to-year variability in occurrence dates of LSF events and the variability in the spring series (FMAM) of the (a) NAO and (b) AO indices

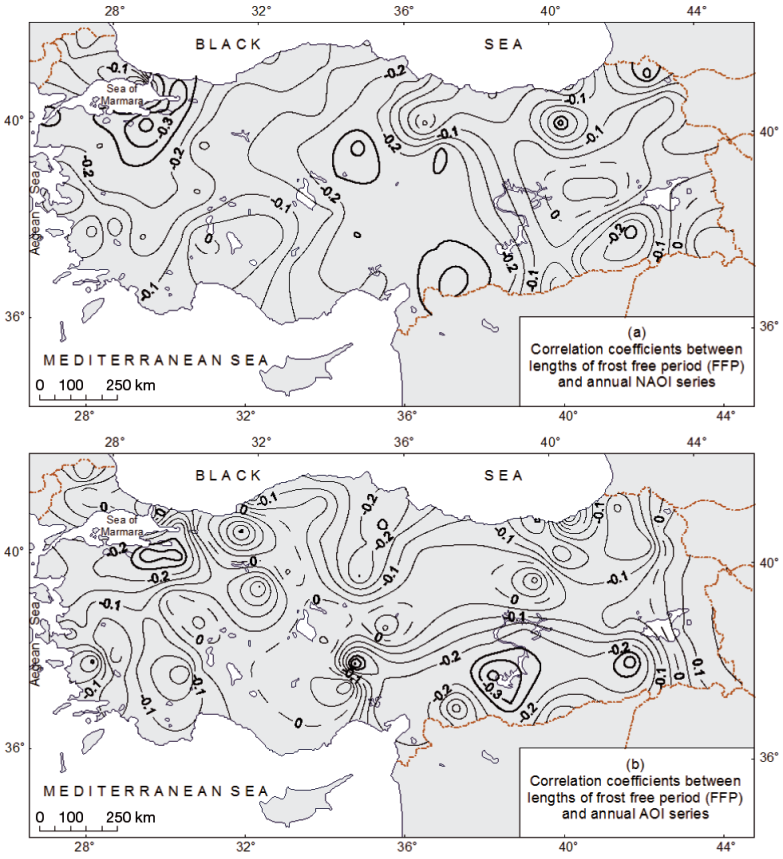

Fig. 9. Geographical distribution patterns of correlation coefficients between the year-to-year variability in FFP and the variability in the annual series the (a) NAO and (b) AO indices

ranean Basin. Consequently, many previous studies also depicted that the influence of the NAO and AO variability is more pronounced in the winter half-year, and weakens and disappears as summer advances (e.g. Xoplaki et al. 2003, Ziv et al. 2004, Tatli et al. 2005, Türkeş & Erlat, 2008, 2009, etc.).

4.2. Anomalous atmospheric patterns connected with extreme dates of frost events in Turkey

In order to further examine the influences of the NAO/AO teleconnections and anomalous circulation patterns associated with the occurrence of extreme dates of the FFF and LSF events (i.e. earliest or latest) in Turkey, we calculated the northern hemispheric scale composite anomalies of both 500 hPa standard pressure level geopotential heights (m), meridional and zonal wind speeds (m s^{-1}), and 850 hPa standard pressure level air temperatures (°C). We chose the 500 hPa geopotential height level heights and meridional and zonal winds approximately 5.5 km above sea level as a governing level for this analysis, because the upper atmospheric conditions at these level closely lead and control the weather systems beneath; in particular, dynamical weather systems move approximately in the same direction as the winds at the 500 hPa level (Türkeş 2010). Geopotential height contours reveal the main tropospheric waves (i.e. Rossby waves) that lead and control the weather state or a weather circulation type over a geographical area. Lower geopotential heights correspond to atmospheric troughs and lows (cyclones), whereas higher geopotential heights reveal atmospheric ridges and highs (anticyclones) in the middle troposphere. If these are dynamically originated deep systems, the middle tropospheric troughs and low centres (cyclones) are closely associated with the surface troughs or squall lines and frontal low pressure systems (i.e. mid-latitude cyclones), whilst the middle tropospheric ridges and high centres (anticyclones) are closely linked to the surface high pressure ridges and high pressure systems. We also studied the anomaly patterns of the 850 hPa standard pressure level air temperatures (°C) approximately 1.5 km above sea level, which is just above the atmospheric boundary layer, because air temperatures at 850 hPa level depict cold and warm air advections, particularly the areas of large air temperature gradients, and thus the frontal zones, where the isotherms are more closely packed together, marking the boundary between relatively warm and cold air masses (Türkeş 2010).

The years used for the atmospheric composite analysis were those when earliest and latest FFF and LSF events were recorded at the majority of stations; specifically those with the 5 latest and 5 earliest FFF dates in the fall season, and the 4 earliest and 5 latest LSF dates in the spring season.

4.2.1. Latest FFF dates in the years 1952, 1960, 1966, 2009 and 2012

We applied atmospheric composite analysis to the 5 years when the 5 latest FFF dates were recorded at most of the stations, i.e. 1952, 1960, 1966, 2009 and 2012. These years corresponded mostly to extreme and normal low index years of the NAO and AO indices in autumn. Composite 500-hPa geopotential height anomalies patterns for those years indicate

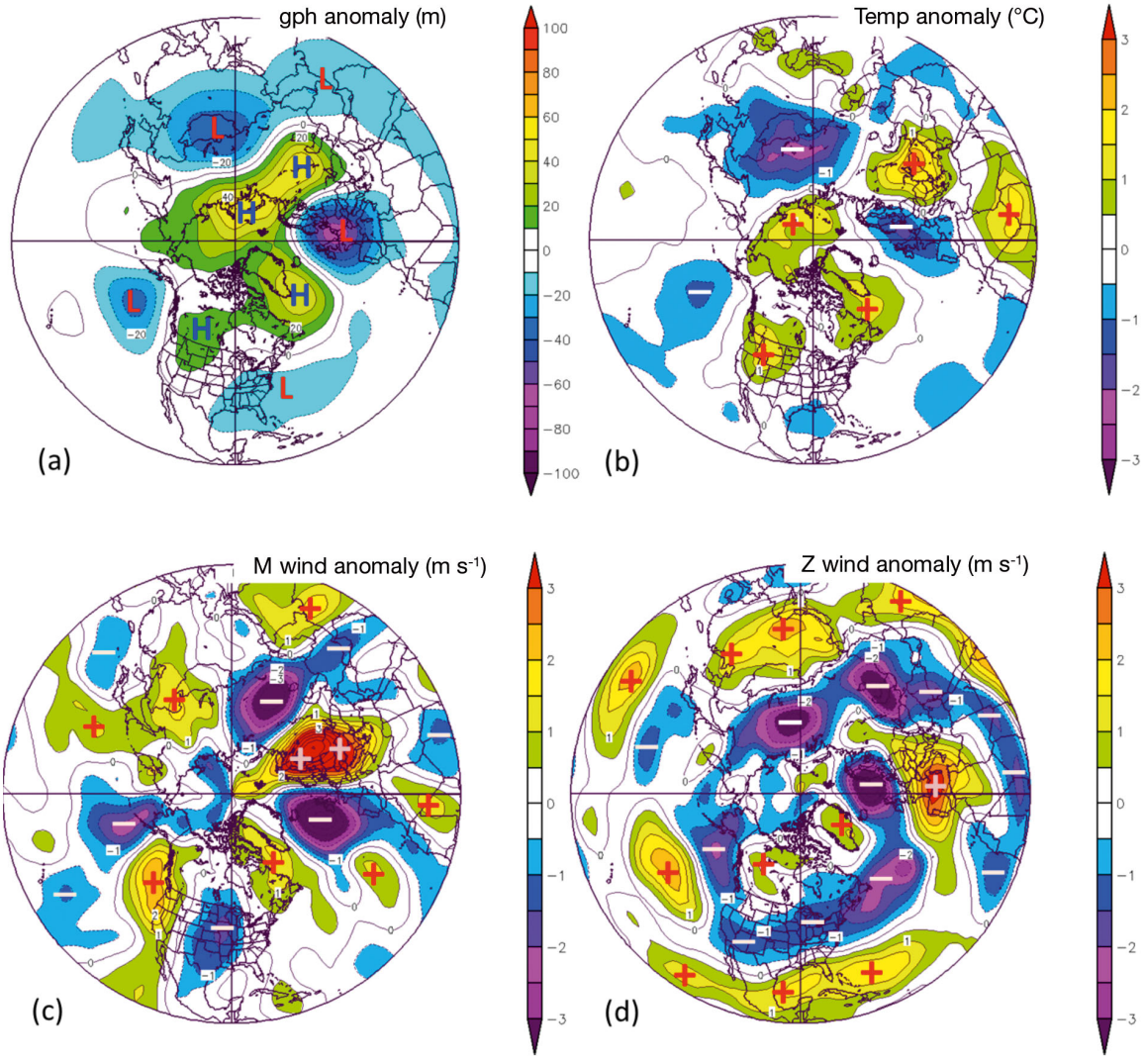

Fig. 10. Northern hemispheric atmospheric anomaly patterns based on (a) 500 hPa geopotential height standard pressure level (m), (b) 850 hPa standard pressure level air temperatures (°C), and 500 hPa (c) meridional and (d) zonal winds (m s^{-1}) for years in which latest first fall frost (FFF) dates were recorded in Turkey. Composite anomalies for the September to December period are calculated as departures from the 1981–2010 base period climatology for the years 1952, 1960, 1966, 2009 and 2012

the presence of anticyclonic anomaly centres over a large area, from Greenland, the Davis Strait, the Labrador Sea and the mid-Arctic Ocean over Europe as far as the Central Mediterranean Basin and the northwestern part of Turkey, and of a deep cyclonic anomaly centre over the northwestern part of Europe (Fig. 10a). Positioning of the anticyclonic geopotential height anomalies over the north of Turkey enables a stagnant surface weather pattern over Turkey to develop, causing somewhat stable atmospheric conditions. During this phase, meridional winds at the 500 hPa level are stronger than long-term average conditions, while zonal winds are weaker over the Middle East, southwestern Asia and most parts of Turkey (Fig. 10c,d). This combined anomalous synoptic pattern clearly supports the occurrence of air temperature conditions warmer than long-term averages over most of Turkey during the autumn seasons of those years. Air temperature anomalies at the 850 hPa level reveal a 1.5 to 2°C positive (warmer) departure from normal especially over the northeastern part of the Anatolian Peninsula (Fig. 10b).

4.2.2. Earliest FFF dates in the years 1953, 1956, 1965, 1973 and 1995

By contrast, the 5 earliest FFF events at most of the stations in Turkey occurred in the years 1953, 1956, 1965, 1973 and 1995. The corresponding pattern of

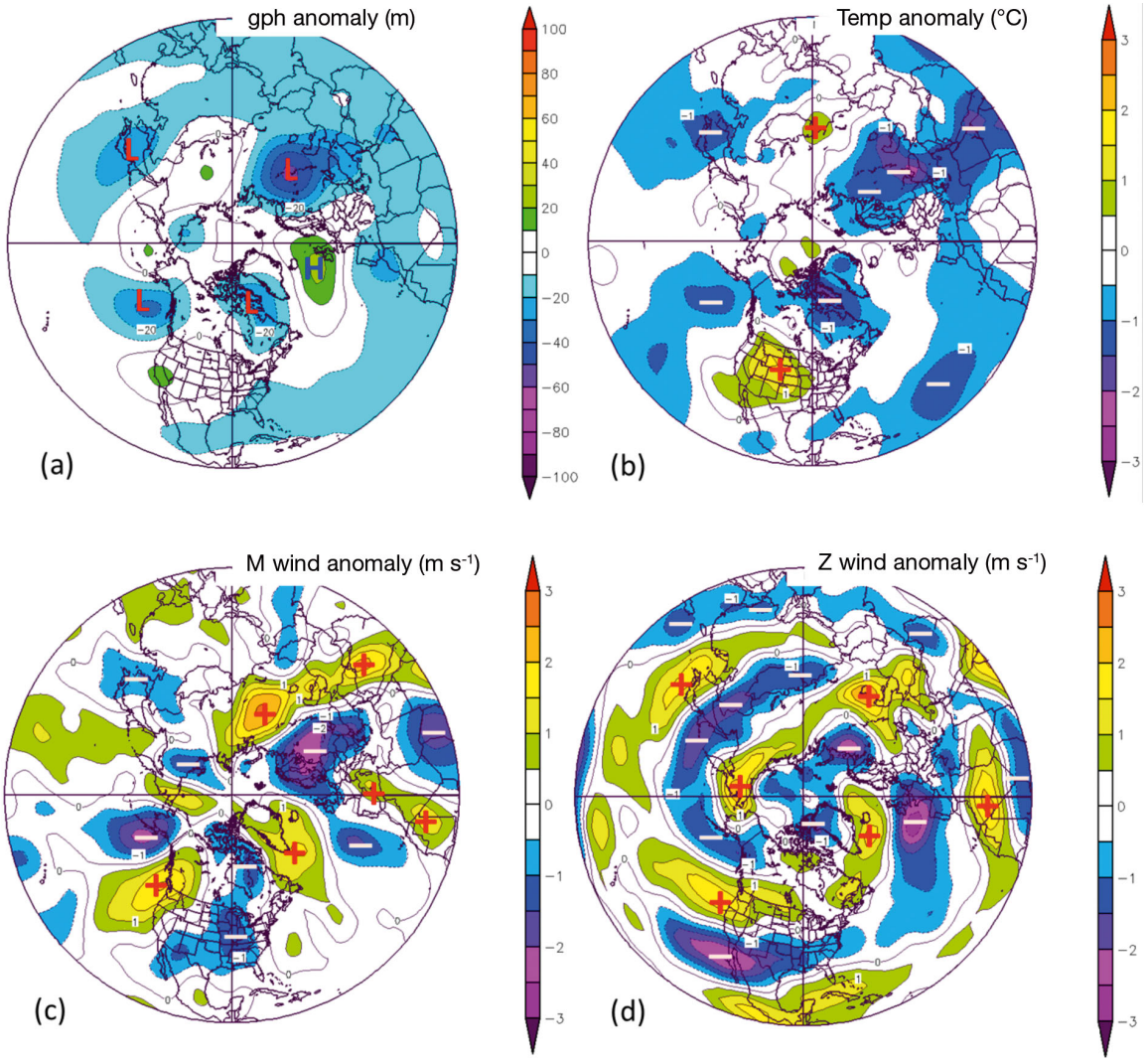

Fig. 11. Northern hemispheric atmospheric anomaly patterns based on (a) 500 hPa geopotential height (m), (b) 850 hPa standard pressure level air temperatures (°C), and 500 hPa (c) meridional and (d) zonal winds (m s^{-1}) for years in which earliest first fall frost (FFF) dates were recorded in Turkey. Composite anomalies for the September to December period are calculated as departures from the 1981–2010 base period climatology for the years 1953, 1956, 1965, 1973 and 1995

composite 500 hPa geopotential height anomalies in those years shows occurrence of the lower than long-term average geopotential height conditions across the Labrador Sea, Japan, and particularly over the wider region of Northern and Eastern Europe and Russia, towards Turkey (Fig. 11a). The deeper cyclonic anomaly centre, with a trough-shaped extension from Northern Europe and Russia to the Black Sea Basin and Turkey, produces surface air temperatures colder than long-term averages in Turkey. Air temperature anomalies at the 850 hPa level show 2 to 3°C negative (colder) departures especially over southwest Asia, and 1 to 2°C cold anomalies over Turkey and the Middle East regions towards the Arabian Peninsula (Fig. 11b). Below normal surface and 850 hPa level air temperature conditions over Turkey and in this broader region are coincident with an anomalous 500 hPa level meridional wind pattern (Fig. 11c). This pattern may also be related to the weakening of the zonal wind circulation over the Mid-Atlantic, Western and Central Mediterranean basins towards Turkey (Fig. 11d).

4.2.3. Earliest LSF dates in the years 1951, 2001, 2008 and 2013

LSF events occurred earlier than average in the years 1951, 2001, 2008 and 2013. The 4 years listed also corresponded to overall normal to extreme nega-

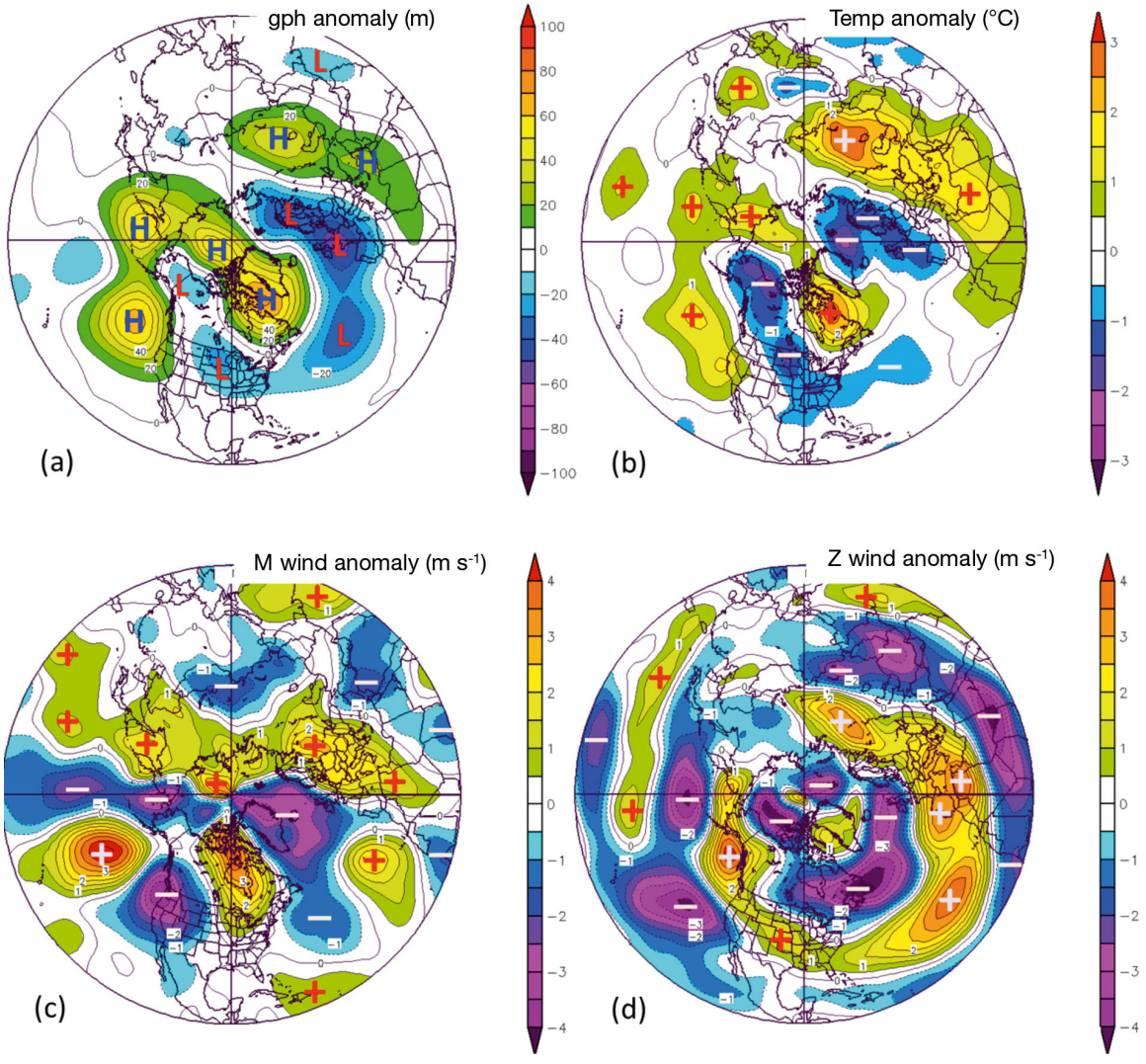

Fig. 12. Northern hemispheric atmospheric anomaly patterns based on (a) 500 hPa geopotential height (m), (b) 850 hPa standard pressure level air temperatures (°C), and 500 hPa (c) meridional and (d) zonal winds (m s^{-1}) for years in which earliest last spring frost (LSF) dates were recorded in Turkey. Composite anomalies for the March to May period are calculated as departures from the 1981–2010 base period climatology for the years 1951, 2001, 2008 and 2013

tive phases of the AO and NAO variability regimes. Atmospheric anomaly patterns of these years are characterised by a strong negative geopotential height anomaly at the 500 hPa level over the North Atlantic including the Labrador Sea (west of Greenland) and Icelandic regions and Europe. Conversely, a positive geopotential height anomaly ridge occurs over Northern Africa, the Eastern Mediterranean Basin and Middle East regions extending up to mid-western and Central Asia regions (Fig. 12a). There are geopotential heights that are anomalously below normal located over the North Atlantic centred over Scandinavia and the Northern Europe regions at these times.

Positioning of the increased geopotential height anomalies enhances and controls the anomalous anticyclonic circulation and atmospheric stability over Turkey. Consequently, this pattern may also maintain lower amounts of cloud cover in Turkey and surrounding regions, leading to a net positive effect on the radiation/energy balance of the surface, mainly due to increased amounts of insolation during the day. The larger regions characterised with marked 500 hPa level cyclonic anomalies, including the area located in the western part of Turkey and over the northern Mediterranean zone are also under the influence of spatially coherent and markedly increased 500 hPa meridional and zonal wind circulations (Fig. 12c,d). It

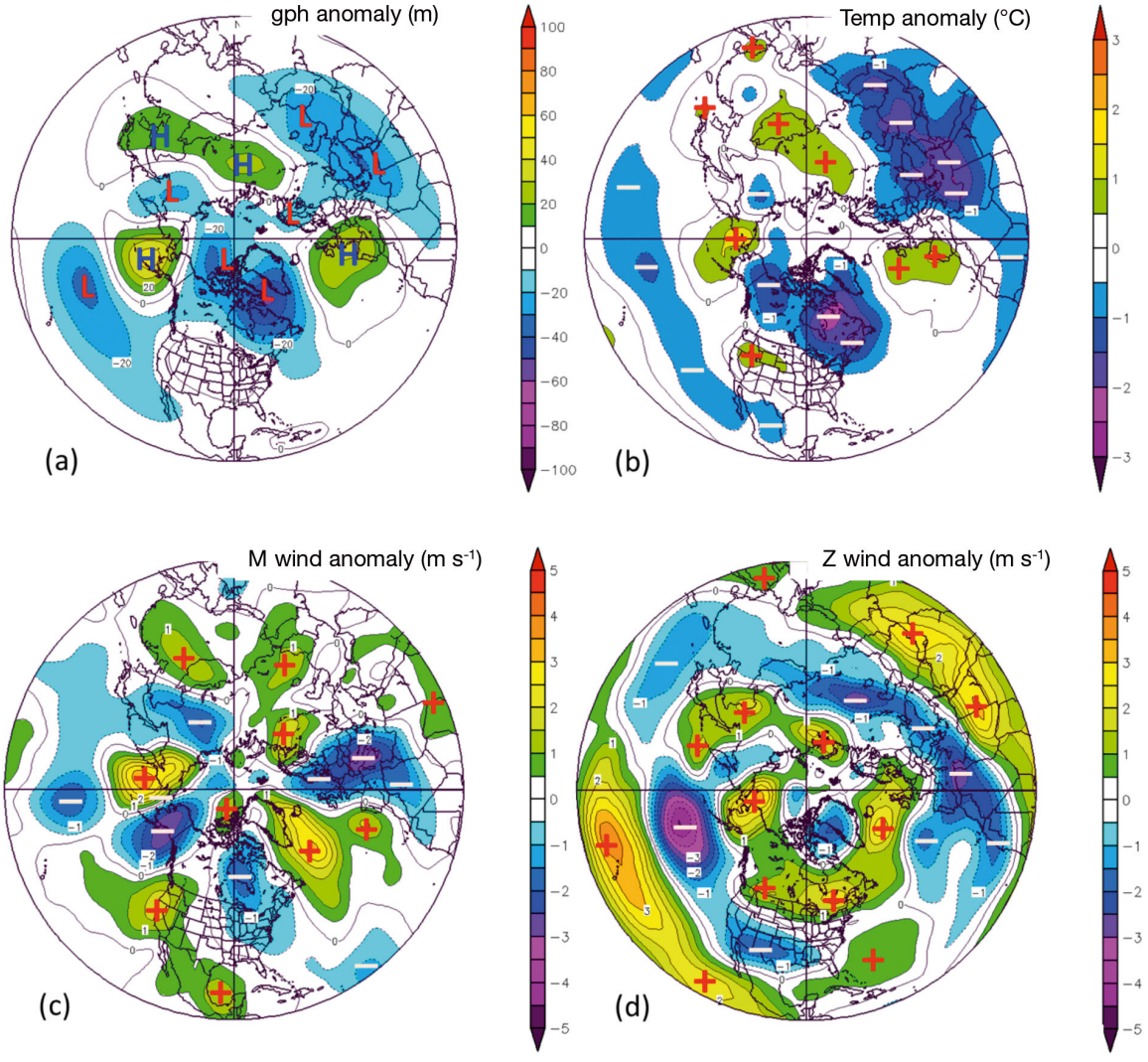

Fig. 13. Northern hemispheric atmospheric anomaly patterns based on (a) 500 hPa geopotential height (m), (b) 850 hPa standard pressure level air temperatures (°C), and 500 hPa (c) meridional and (d) zonal winds (m s^{-1}) for years in which latest last spring frost (LSF) dates were recorded in Turkey. Composite anomalies for the March to May period are calculated as departures from the 1981–2010 base period climatology for the years 1967, 1987, 1992, 1997 and 2003

is also notable that the observed anomalous zonal winds at the 500 hPa level exhibit a very strong and spatially coherent zonal (elongated west to east) negative anomaly pattern extending from Africa towards Pakistan and India (Fig. 12d). In addition to a tendency towards higher geopotential heights, including a warm high pressure ridge over Turkey, the anomalous meridional and zonal circulation patterns described above may contribute to the occurrence of air temperature conditions that are warmer than long-term average, at the 850 hPa standard pressure level. Composite air temperature anomalies at the 850 hPa level are about 1 to 2°C warmer over Turkey relative to the 1981 to 2010 normal (Fig. 12b).

4.2.4. Latest LSF dates in the years 1967, 1987, 1992, 1997 and 2003

Fig. 13 shows the northern hemispheric spring season composite atmospheric anomaly patterns for the years 1967, 1987, 1992, 1997 and 2003 with respect to the 1981–2010 climatology. These years are characterised by later dates for LSF events at many stations. Composite anomalies for years associated with the 5 latest dates of LSF exhibit normal to extreme positive phases of the AO/NAO regime. The observed 500 hPa composite geopotential height anomalies for the spring months of these years reveal the presence of strong negative (i.e. deep cyclonic) anomaly pat-

terns over both North America and to the west of Greenland, and somewhat weak negative anomalies occurred over the Middle East, Iran, Pakistan and the Eastern Mediterranean Basin including Turkey (Fig. 13a).

Anomalous cold temperature advection throughout Turkey at the 850 hPa level may have be linked both to the 500 hPa level composite negative meridional wind anomalies over Western and Central Europe and the Mediterranean Basin, and an anomalous zonal pattern of negative zonal wind circulation dominating over a large area from the eastern Mid-Atlantic to Central and South Asia via the Mediterranean Basin and Turkey (Fig. 13c,d). Combinations of those atmospheric anomalous patterns resulted in 1 to 2°C negative temperature anomalies at the 850 hPa level air temperatures relative to the 1981–2010 climatology over the larger region extending from the Balkans, Eastern Mediterranean and Black Sea basins and Turkey to Pakistan via the Middle East and Iran (Fig. 13b).

5. SUMMARY AND CONCLUSIONS

Global datasets of daily T_{min} and T_{max} air temperatures showed that the statistical distribution shapes of the global T_{min} and T_{max} series have shifted towards warmer temperatures over the past 60 yr (IPCC 2013). Greater changes have been reported for T_{min} than for T_{max} since the middle of the 20th century (Donat et al. 2012). By considering the results of many recent studies and the IPCC's Fifth Assessment Report (IPCC 2013), we would further suggest for Turkey that changes in the occurrence dates of the FFF and LSF events may have resulted in the extension of the FFP lengths.

The time series of average dates of the LSF and the FFF events as well as the length of the FFP showed high interannual variability and some apparent periods characterised by distinct variability regimes. All frost event indices exhibited pronounced changes around the mid-1990s. From this time onwards, dates of FFF were later and LSF occurred earlier, leading to an increase in the length of FFPs at most stations, although some regional differences are evident in trend characteristics, particularly in the Black Sea. Observed trends in all regional frost event series of the BLS Region are opposite to the trend patterns detected for the rest of Turkey. Findings also indicated that these observed changes in most of Turkey have been stronger over recent decades. Ordinary LSLR analysis applied to the annual averages of Turkey as a whole also revealed that the LSF occurred earlier by −0.64 d per decade, while the FFF occurred +0.1 d per decade later. As a result, FFP was lengthened +0.71 d per decade over the study period.

The majority of climatological and phenological studies showed a lengthening of the frost free period (and therefore also the growing season) in the last few decades due to the marked change of LSF dates (e.g. Frich et al. 2002, Ahas et al. 2002, Menzel et al. 2003, Scheifinger et al. 2003, etc.). Our time-series analysis also suggested that the FFP lengthened mainly as a result of both earlier LSP and later FFF in Turkey. The results of the Mann–Kendall test showed that the frost-free period was evidently longer at 40 stations due to both later dates of FFF and the earlier dates of LSF. The length of FFP increased at 12 stations due to earlier dates of LSF. On the other hand, 6 stations showed non-significant increasing trends in the FFP where FFF occurred later. Correlation analysis revealed that some of the variability associated with FFF, LSF dates and length of FFP may be explained by the variability of large-scale atmospheric circulation patterns like AO and NAO. We also found a strong negative connection between the variability of FFF dates and large-scale atmospheric oscillations. On the other hand, there is a positive correlation between the dates of the LSF events and AO/NAO spring indices.

It is evident that the phase of the AO has a greater influence on dates of FFF than the NAO phase. Regarding the linkage between the LSF dates and the large-scale circulation patterns, the NAO proved to be the most influential in spring. There is a weak inverse relationship between lengths of the FFP and both NAO and AO annual indices.

Anomalous patterns of 500 hPa level geopotential heights, zonal and meridional winds, and 850 hPa level air temperatures were also examined, and compared with the composites for the years characterized by earliest/latest dates of FFF and LSF over most of Turkey. Composite years of earlier FFF and latest LSF dates were associated with a strong negative anomaly over the Eastern Mediterranean Basin and Turkey, and with a cold air advection observed at the 850 hPa level. On the other hand, the years that featured later (earlier) FFF (LSF) dates than long-term averages across Turkey were accompanied by a strong positive geopotential height at the 500 hPa level. The ridge of high pressure at 500 hPa level that was centred over the Eastern Mediterranean Basin and Turkey may maintain the advection of warm air into the surface high pressure zone.

Acknowledgements. We thank Dr. Matthew Jones (School of Geography, University of Nottingham) for English editing to improve our manuscript and for his valuable comments, and the anonymous reviewers who offered valuable suggestions and constructive comments on the manuscript. We thank the NOAA Earth System Research Laboratory, Physical Sciences Division for providing the R1 dataset, and their Senior Associate Scientist Ms. Cathy Smith for guidance in selecting and comparing the reanalysis datasets used in the paper.

LITERATURE CITED

Ahas R, Aasa A, Menzel A, Fedotova VG, Scheifinger H (2002) Changes in European spring phenology. Int J Climatol 22:1727–1738

Altinsoy H, Öztürk T, Türkeş M, Kurnaz ML (2012) Simulating the climatology of extreme events for the central Asia domain using the RegCM 4.0 regional climate model. In: Helmis CG, Nastos P (eds) Advances in meteorology, climatology and atmospheric physics. Springer, Berlin, p 365–370

Bartholy J, Pongrácz R (2007) Regional analysis of extreme temperature and precipitation indices for the Carpathian Basin from 1946 to 2001. Global Planet Change 57:83–95

Beniston M, Stephenson DB, Christensen OB, Ferro CAT and others (2007) Future extreme event in European climate: an exploration of regional climate model projections. Clim Change 81:71–95

Castro-Diez Y, Pozo-Vazquez D, Rodrigo FS, Esteban-Parra MJ (2002) NAO and winter temperature variability in southern Europe. Geophys Res Lett 29, doi:10.1029/2001GL014042

Donat MG, Alexander LV, Yang H, Durre I and others (2013) Updated analyses of temperature and precipitation extreme indices since the beginning of the twentieth century: the HadEX2 dataset. J Geophys Res Atmos 118: 2098–2118

Easterling DR, Horton B, Jones PD, Peterson TC and others (1997) Maximum and minimum temperature trends for the globe. Science 277:364–367

Erlat E, Türkeş M (2012) Analysis of observed variability and trends in numbers of frost days in Turkey for the period 1950–2010. Int J Climatol 32:1889–1898

Fahmi F, Kartal E, İyigun C, Türkeş M and others (2007) Determining the climate zones of Turkey by center-based clustering methods. In: Tenreiro Machado JA, Baleanu D, Luo A (eds) Nonlinear dynamics of complex systems: applications in physical, biological and financial systems. Springer, Berlin, p 171–178

Frich P, Alexander LV, Della-Marta P, Gleason B, Haylock M, Klein Tank AMG, Peterson T (2002) Observed coherent changes in climatic extremes during the second half of the twentieth century. Clim Res 19:193–212

Giorgi F, Lionello P (2008) Climate change projections for the Mediterranean region. Global Planet Change 63: 90–104

Hansen J, Sato M, Ruedy R (2012) Perception of climate change. P Natl Acad Sci USA 109:E2415–E2423

IPCC (2013) Climate change 2013: the physical science basis. Contribution of Working Group I to the Fifth Assessment Report of the Intergovernmental Panel on Climate Change. Cambridge University Press, Cambridge

Iyigün C, Türkeş M, Batmaz İ, Yozgatlıgil C, Gazi VP, Koç EK, Öztürk MZ (2013) Clustering current climate regions of Turkey by using a multivariate statistical method. Theor Appl Climatol 114:95–106

Kalnay E, Kanamitsu M, Kistler R, Collins W and others (1996) The NCEP/NCAR 40-year reanalysis project. Bull Am Meteorol Soc 77:437–471

Kirbyshire AL, Bigg GR (2010) Is the onset of the English summer advancing? Clim Change 100:419–431

Klein Tank AMG, Können GP (2003) Trends in indices of daily temperature and precipitation extremes in Europe, 1946–99. J Clim 16:3665–3680

Kuglitsch FG, Toreti A, Xoplaki E, Della-Marta PM, Zerefos CS, Türkeş M, Luterbacher J (2010) Heat wave changes in the eastern Mediterranean since 1960. Geophys Res Lett 37:L04802, doi:10.1029/2009GL041841

Kutiel H, Türkeş M (2005) New evidence for the role of the North Sea — Caspian Pattern on the temperature and precipitation regimes in continental central Turkey. Geogr Ann A 87:501–513

Menzel A, Fabian P (1999) Growing season extended in Europe. Nature 397:659

Menzel A, Jakobi G, Ahas R, Scheifinger H, Estrella N (2003) Variations of the climatological growing season (1951–2000) in Germany compared with other countries. Int J Climatol 23:793–812

Orlowsky B, Seneviratne SI (2012) Global changes in extreme events: regional and seasonal dimension. Clim Change 110:669–696

Öztürk T, Ceber ZP, Türkeş M, Kurnaz ML (2015) Projections of climate change in the Mediterranean Basin by using downscaled global climate model outputs. Int J Climatol 35:4276–4292

Qian C, Fu C, Wu Z, Yan Z (2009) On the secular change of spring onset at Stockholm. Geophys Res Lett 36:L12706, doi:10.1029/2009GL038617

Şahin S, Cigizoglu HK (2012) The sub-climate regions and the sub-precipitation regime regions in Turkey. J Hydrol (Amst) 450–451:180–189

Scheifinger H, Menzel A, Koch E, Peter C (2003) Trends of spring time frost events and phenological dates in Central Europe. Theor Appl Climatol 74:41–51

Smith CA, Compo GP, Hooper DK (2014) Web-based Reanalysis Intercomparison Tools (WRIT) for analysis and comparison of reanalyses and other datasets. B Am Meteorol Soc 95:1671–1678

Sneyers R (1990) On the statistical analysis of series of observations. Technical Note 143, World Meteorological Organization, Geneva

Tatli H, Dalfes N, Mente S (2005) Surface air temperature variability over Turkey and its connection to large-scale upper air circulation via multivariate techniques. Int J Climatol 25:331–350

Türkeş M (1998) Influence of geopotential heights, cyclone frequency and southern oscillation on rainfall variations in Turkey. Int J Climatol 18:649–680

Türkeş M (2010) Climatology and meteorology, 1st edn. Physical Geography Series No. 1, Kriter Publishing, Istanbul (in Turkish)

Türkeş M (2013) Observed and projected climate change, drought and desertification in Turkey. Ankara Üniversitesi Çevre Bilimleri Dergisi 4:1–32 (in Turkish with English abstract)

Türkeş M, Erlat E (2008) Influence of the Arctic Oscillation on variability of winter mean temperatures in Turkey. Theor Appl Climatol 92:75–85

Türkeş M, Erlat E (2009) Winter mean temperature variability in Turkey associated with the North Atlantic Oscillation. Meteorol Atmos Phys 105:211–225

Türkeş M, Sümer UM (2004) Spatial and temporal patterns of trends and variability in diurnal temperature ranges of Turkey. Theor Appl Climatol 77:195–227

Türkeş M, Sümer UM, Demir Í (2002a) Re-evaluation of trends and changes in mean, maximum and minimum temperatures of Turkey for the period 1929–1999. Int J Climatol 22:947–977

Türkeş M, Sümer UM, Kılıç G (2002b) Persistence and periodicity in the precipitation series of Turkey and associations with 500 hPa geopotential heights. Clim Res 21: 59–81

Turp MT, Öztürk T, Türkeş M, Kurnaz, ML (2015) Assessment of projected changes in air temperature and precipitation over the Mediterranean region via multi-model ensemble mean of CMIP5 models. J. Black Sea/Mediterranean Environ Spec Issue 21:93–96.

WMO (1966) Climatic change. Technical Note 79, World Meteorological Organization, Geneva

Xoplaki E, González-Rouco JF, Luterbacher J, Wanner H (2003) Mediterranean summer air temperature variability and its connection to the large-scale atmospheric circulation and SSTs. Clim Dyn 20:723–739

Yao Y, Luo D (2014) Relationship between zonal position of the North Atlantic Oscillation and Euro-Atlantic blocking events and its possible effect on the weather over Europe. Sci China Earth Sci 57:2628–2636

Zhang X, Aguilar E, Sensoy S, Melkonyan H and other (2005) Trends in Middle East climate extreme indices from 1950 to 2003. J Geophys Res Atmos 110:D22104, doi:10.1029/2005JD 006181.

Ziv B, Saaroni H, Alpert P (2004) The factors governing the summer regime of the eastern Mediterranean. Int J Climatol 24:1859–1871

Editorial responsibility: Oliver Frauenfeld, College Station, Texas, USA

Submitted: October 5, 2015; Accepted: April 12, 2016
Proofs received from author(s): June 29, 2016